Leap-dynamics: efficient sampling of conformational space of proteins and peptides in solution

Jens Kleinjung[a,*], Peter Bayley[a], Franca Fraternali[b]

[a] *Physical Biochemistry Division, National Institute for Medical Research, Mill Hill, London NW7 1AA, UK*
[b] *Molecular Structure Division, National Institute for Medical Research, Mill Hill, London NW7 1AA, UK*

Received 10 January 2000; received in revised form 21 February 2000

Edited by Matti Saraste

Abstract A molecular simulation scheme, called Leap-dynamics, that provides efficient sampling of protein conformational space in solution is presented. The scheme is a combined approach using a fast sampling method, imposing conformational 'leaps' to force the system over energy barriers, and molecular dynamics (MD) for refinement. The presence of solvent is approximated by a potential of mean force depending on the solvent accessible surface area. The method has been successfully applied to *N*-acetyl-L-alanine-*N*-methylamide (alanine dipeptide), sampling experimentally observed conformations inaccessible to MD alone under the chosen conditions. The method predicts correctly the increased partial flexibility of the mutant Y35G compared to native bovine pancreatic trypsin inhibitor. In particular, the improvement over MD consists of the detection of conformational flexibility that corresponds closely to slow motions identified by nuclear magnetic resonance techniques.

Key words: Molecular dynamics; Sampling; Implicit solvent; Protein motion

1. Introduction

Protein dynamics involving conformational equilibria and folding processes occurs on a great variety of time scales ranging from picoseconds to minutes [1]. Computer simulations can provide an important insight into protein folding mechanisms. However, even the most extensive molecular dynamics (MD) simulation, spanning 1 μs of a small protein folding in water [2], can only supply a partial picture of the complex folding process. An alternative to long-term MD is complete mapping of the protein energy landscape by theoretical or experimental methods. This would effectively solve the protein folding problem and at the same time allow for a detailed description of protein dynamics. However, such a complete mapping is not feasible [3] and current techniques provide only limited information on the energy landscape. A given protein structure explores multiple conformations close to the lowest possible free energy, all of which exhibit very similar structural characteristics. Conformational substates also exist, which are separated by energy barriers larger than $k_B T$ (where k_B is the Boltzmann constant and T is the temperature). Transitions between substates occur on relatively long time scales [4]. Therefore, it is of central importance to develop time-saving techniques, which allow for an improved sampling of configurational space [5,6]. Several approaches have recently been proposed to enhance the efficiency of the exploration of configurational space [7–10]. It has been concluded that the future of sampling methods relies on multiple approaches using a combination of fast sampling methods and MD to obtain a realistic ensemble [11,12].

Here, a combined approach of MD and the CONCOORD 'essential dynamics' method (CED) [9] is proposed, which we call Leap-dynamics (LD). LD uses CED to impose conformational perturbations of the molecule that are sufficient to force the system over energy barriers, allowing access to different regions of the energy surface. To refine individual sampled conformations, the molecule is then allowed to relax to lower energy states through application of MD in implicit solvent [13]. LD has been tested on two model systems: *N*-acetyl-L-alanine-*N*-methylamide (alanine dipeptide) and bovine pancreatic trypsin inhibitor (BPTI). Alanine dipeptide is used to examine the ability of LD to sample a full conformational energy space for a small molecule. BPTI is used to examine the ability of LD to simulate the effect of a destabilising mutation on the molecular flexibility of a small protein, in particular the increase in conformational space accessible to the mutant protein.

Alanine dipeptide has been used for many theoretical studies as a minimum model containing a single ϕ/ψ angle pair. An ab initio study has calculated the energy profile of the complete ϕ/ψ map in vacuo [14]. Low-energy conformations are found in the $C7_{eq}$, C5, β and P_{II} region (herein referred to as β region) and in the α_R region. However, solvent interactions play an important role in determining the conformations of the peptide. A combined CD and nuclear magnetic resonance (NMR) study showed a conformational transition from preferentially $C7_{eq}$ in apolar solvents to preferentially P_{II} and α_R in polar/aqueous solution [15]. Previous results using a Langevin/implicit-Euler scheme successfully improved the sampling of β and α_R conformations in vacuo with respect to simple MD [16]. A successful sampling method should detect conformations spanning the β and α_R regions and it should include solvent contributions.

BPTI represents a model system for method developments on proteins. Numerous studies by crystallography [17], NMR [18–20] and molecular simulation [20–23] have been per-

*Corresponding author. Fax: (44)-208-906 4477.
E-mail: jkleinj@nimr.mrc.ac.uk

Abbreviations: BPTI, bovine pancreatic trypsin inhibitor; CED, CONCOORD 'essential dynamics'; EM, energy minimisation; LD, Leap-dynamics; MD, molecular dynamics; NMR, nuclear magnetic resonance; rmsd, root mean square deviation

PII: S0014-5793(00)01295-3

formed in order to characterise the structural and dynamic properties of this molecule. The mutant Y35G BPTI represents an interesting example in which a single point mutation enhances significantly the flexibility of 40% of the residues as shown by means of crystallography [24] and NMR investigations [25].

2. Materials and methods

2.1. Simulation methods

Calculations were performed on Intel PII processors (350 and 400 MHz) running on the Linux 2.0.36 kernel. The atomic coordinates of the crystal structures of the model structure BPTI (1BPI) [26] and Y35G BPTI (8PTI) [24] were taken from the Brookhaven protein data bank. The GROMOS96 package was used for energy minimisation (EM) and MD simulations [27]. EM was performed using the steepest descent method. MD was run at 300 K applying weak coupling to a temperature bath, using a relative relaxation time of 0.1. The SHAKE algorithm was used, enabling simulated time steps of 2 ps. An implicit solvent was incorporated by a mean force for water interactions [13]. CED simulations were performed by using the program CONCOORD [9]. Secondary structure assessment and hydrogen bond assessment were made by using the program DSSP [28]. Root mean square deviation (rmsd) differences, Ramachandran distributions and angle values were determined using the program MOLMOL [29]. Solvent accessible surface areas were computed by applying self-written routines [13]. The stereochemical quality of structures was checked using the program packages WHATIF [30] and PROCHECK [31].

2.2. LD

LD is performed by passing a structure through sequential cycles of (a) CED, (b) EM, (c) MD and (d) EM simulations. First, a single new structure was generated by CED. This structure was subjected to 50 steps of initial EM, followed by 10 ps of MD in implicit water solvent and further EM for 500 steps. The final structure of one LD cycle was used to initiate the next cycle. This set of parameters was chosen from systematic test simulations. The procedure was automated by software written by the authors.

We have compared the results of LD with separate MD, LD and CED simulations. For alanine dipeptide the separate MD simulation spanned 10 ns and conformations were stored every 10 ps. The LD simulation applied the CED/EM/MD/EM scheme as described above using the same MD routine as the separate MD simulation. The separate CED simulation was used to create 1000 conformations.

Comparative MD, LD and CED simulations were also performed on BPTI and the mutant Y35G BPTI. The separate MD run was performed for 1 ns of molecular motion, storing conformations every 10 ps. The LD simulation applied the CED/EM/MD/EM scheme as described above using the same MD routine as the MD separate simulation. The separate CED simulation was used to generate 100 conformations. Calculation time per cycle (corresponding to the generation of one structure) on a 400 MHz PII processor was about 30 s for alanine dipeptide and 24 min for BPTI or Y35G BPTI.

2.3. Implicit solvation

A recurrent problem in simulations with implicit solvation energy terms is the treatment of ionic sidechains [32]. The balance between polar–non-polar versus non-polar–non-polar group interactions is very different in water and in the gas phase. In the gas phase the two contributions are very similar, while in water desolvating polar groups require energy expenditure and polar–non-polar interactions are consequently repulsive. The solvation mean force approach used here is implemented in combination with the GROMOS96 force field for in vacuo simulations with the total charges of ionic sidechains neutralised (pseudo-ionic sidechains) [13]. This method has been proven to perform well for a number of proteins compared to explicit water simulations. By using implicit solvation in the LD scheme, long equilibration phases of the solvent are avoided. Nevertheless, the introduction of CED steps in each LD cycle perturbs the system more drastically than in a continuous MD simulation, which can produce more unrealistic conformations. In order to avoid this, the implicit solvation was modified with the absolute values of atomic solvation parameters for nitrogen and oxygen atoms of pseudo-ionic sidechains increased about threefold. An alternative modification is to use a distance dependent dielectric constant in combination with the solvation mean force [32].

3. Results and discussion

LD is a combined scheme, applying a sequence of CED/EM/MD/EM to a molecule. The resulting conformation is used as the starting point for the following cycle. The CED step imposes a perturbation by restrained atomic rearrangements ('leaps'), which leads to an average increase in energy. Both factors, the conformational rearrangement (displacement in energy landscape) and the increase in energy (uphill in energy landscape), are essential for overcoming energy barriers. The increase in energy is about 700 kJ/mol, which is 2–3 times the maximum energy fluctuations observed in long-term MD simulations of BPTI [22]. Most of the energy is initially stored in covalent energy terms (bond stretching, angle deformation, dihedral interaction) and these values rapidly decrease during the first EM step in the LD cycle. The MD step relaxes the molecule downhill to a local minimum and thereby refines the structure. In the next sections the application of LD to the chosen systems is shown.

3.1. Alanine dipeptide

The aim is to produce effective sampling of alanine dipeptide conformational space in order to make a direct comparison with MD simulations in implicit water.

The 3D-energy landscape of the alanine dipeptide in explicit water is shown in Fig. 1A. The energy surface in the explicit water simulation is flattened with respect to that obtained in vacuo and the number of local minima is increased, as already pointed out in a previous study which applied a mean force potential for the solvent [33]. The two lowest energy minima correspond to conformations in the β region (close to −80/100) and in the α_R region (close to −60/−60) and they are almost isoenergetic in water. In Fig. 1B–D 2D contour plots of the landscape in Fig. 1A are displayed. The MD run samples only the β region and very poor sampling is achieved in the α_R region. On the other hand, LD successfully samples conformations in both regions. Even though the ϕ/ψ values are slightly spread with respect to the minima of the energy landscape (in water), the sampled conformations clearly populate the two main allowed regions. The observed transition frequency between the β and α_R region is 132 per 1000 generated structures, implying that a major conformational transition is induced about every tenth generated structure. If restraints are applied in order to disallow the α_R region, conformations in the $C7_{ax}$ are found (Fig. 1D). It is important to note that the low energy profile for the α_L region in explicit water simulations (Fig. 1A) is due to particularly favourable water–solute interactions. A bridging water molecule between the two NH amide groups stabilises their proximate disposition in this conformation. In the absence of explicit solvent such a disposition is unfavourable because of electrostatic repulsion of the aligned NH dipoles. This represents a particular case, for which hardly any implicit solvent method could account. Thus, by disallowing the α_R region, the $C7_{ax}$ and α_L regions are accessible by the leaps, but during the early MD relaxation the system tends to escape from the α_L conformers by drifting to the $C7_{ax}$ region. This shows that all main energy

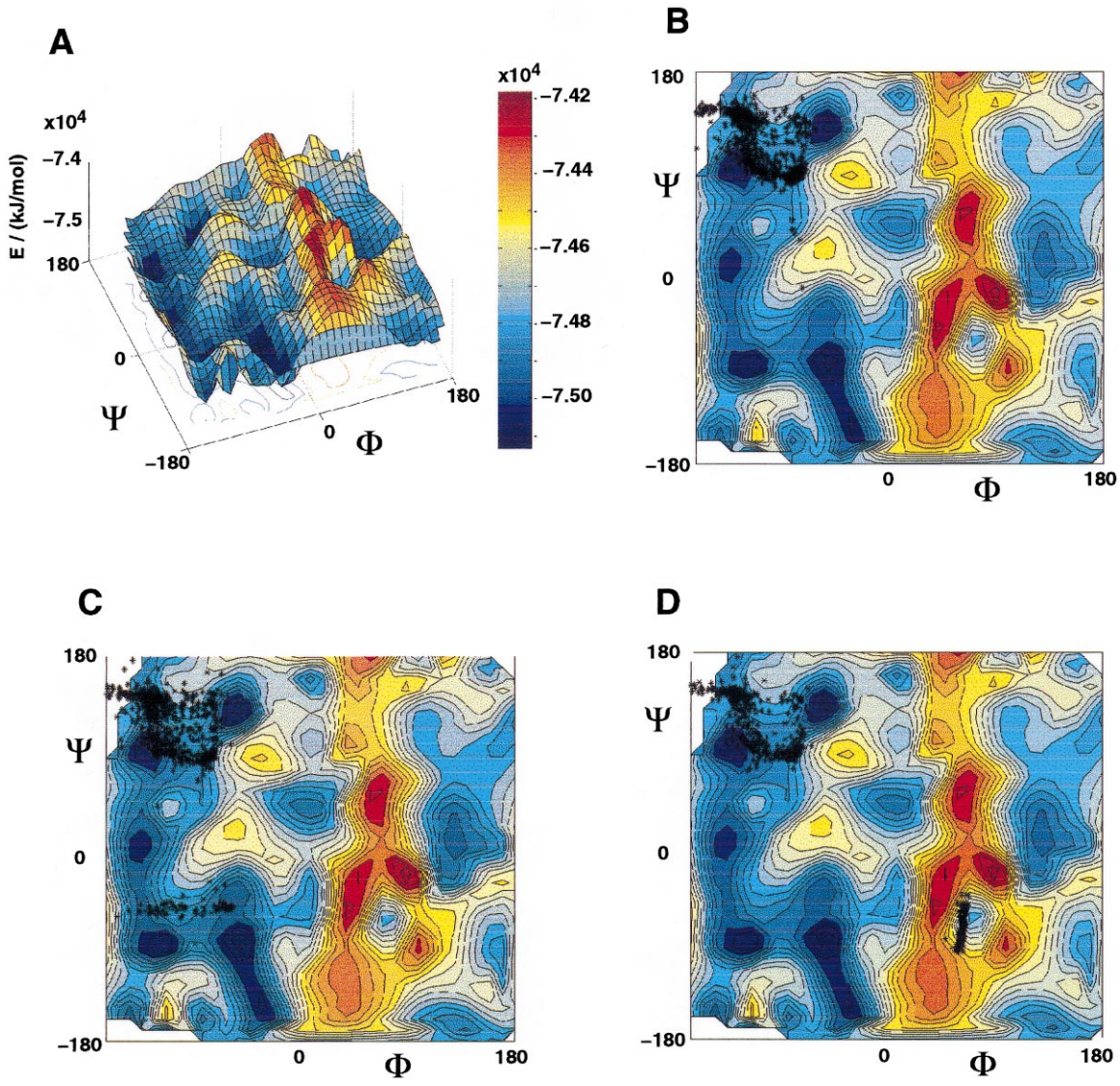

Fig. 1. A: Energy landscape of alanine dipeptide in explicit water. The colour coding is given in the colour bar. B: ϕ/ψ angle pairs (1000) of a 10 ns MD simulation of alanine dipeptide in implicit water are plotted on the projected energy landscape of A (star symbols). MD samples only nearly exclusively in the β region. C: Like B, results from a LD simulation are shown. LD samples in the β and α_R region. D: Like C; LD samples in the β and $C7_{ax}$ region, since the α_R region is disallowed by artificial restraints.

minima are in principle accessible by LD sampling, but $C7_{ax}$ and α_L conformations are less favourable in solvent than α_R, according to experimental findings in water [15].

3.2. BPTI and Y35G BPTI

The performance of the three different methods CED alone, MD alone and LD, with regard to sampling efficiency and quality of generated structures was investigated for the protein BPTI and its Y35G mutant. The results are shown in Fig. 2A,B in which the surface represents the envelope of a bundle of 10 superimposed conformations. Thick regions therefore correspond to high mobility, thin regions to conformationally constrained stretches. All methods show good superimposition of residues in the central region of the molecule and high mobility of the C-terminal residues. However, they clearly differ in the assessment of flexibility in all other parts of the molecule. Results of MD and LD simulations yield similar ranges of mobility for BPTI, whereas CED alone shows flexibility only in loop regions and underestimates the flexibility of other structural elements. The MD and LD simulations of BPTI are very similar since 1 ns of MD samples most of the conformations of the small and rigid protein.

The results for the flexible Y35G mutant show more strikingly the difference in the three methods in assessment of mobility. MD and CED alone show relatively little change in the mobilities of all regions relative to the control BPTI. However, LD reveals the destabilisation of major structural parts by the single-site mutation (Fig. 2B). This is in accordance with evidence of cooperative motion mediated by the 14–38 disulfide bond [34]. The average angle variation (rmsd of ϕ and ψ, see Table 1) between 100 conformations generated by each method and the difference between the two crystal structures is used as a measure of local conformational flexibility [35]. A plot of the angle variation versus the residue number for LD sampling of Y35G is in good agreement with experimental results (Fig. 2C). The same two regions,

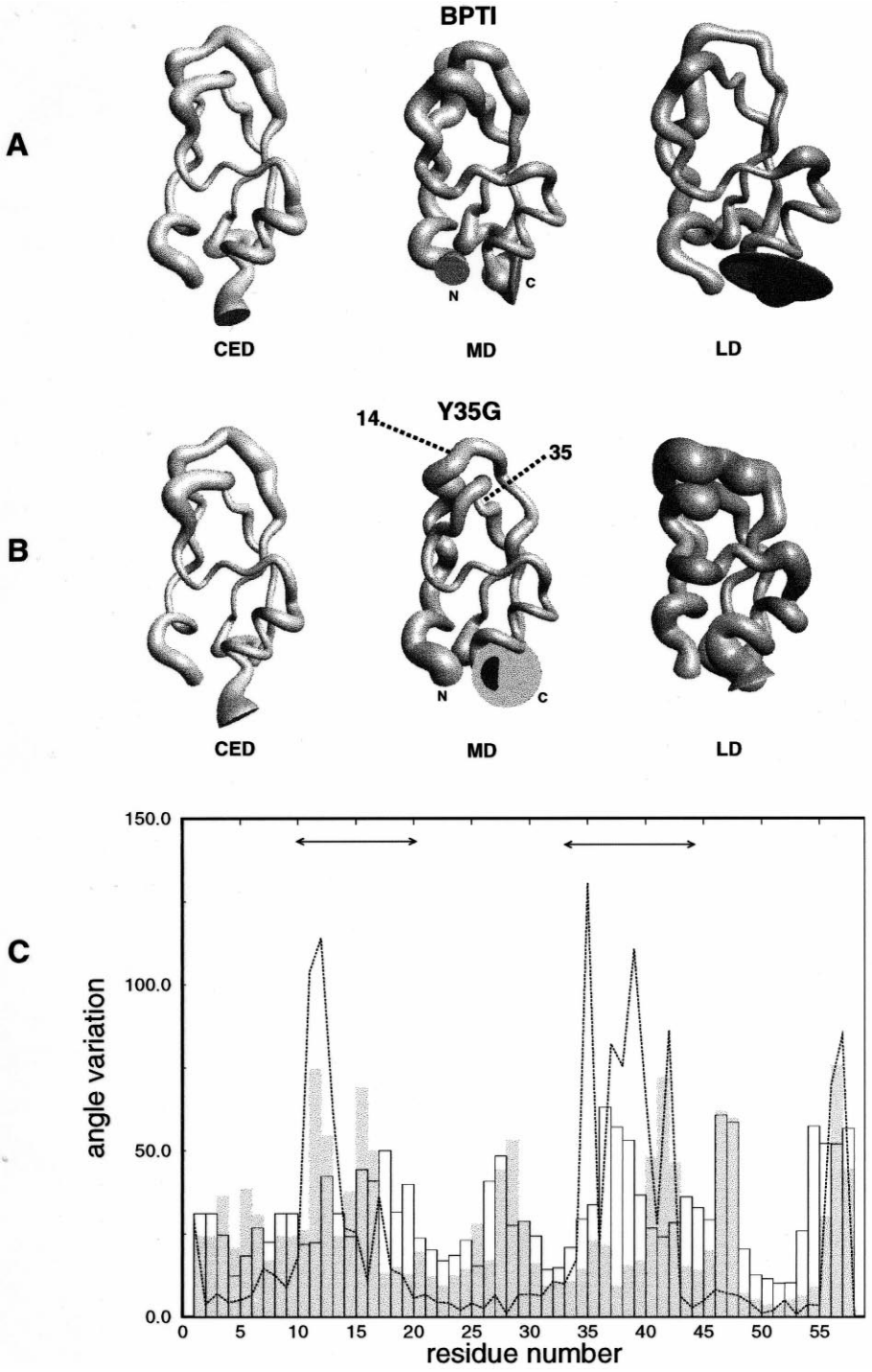

Fig. 2. A and B: Mobility representation of structure bundles of BPTI (A) and Y35G BPTI (B) from CED (left), MD (centre) and LD (right) simulations. Flexible regions are thick, constrained regions are thin. LD samples the increased flexibility of Y35G. The figure was produced using MOLMOL. C: Angle variation of residues in LD simulations of BPTI (gray filled bars) and Y35G BPTI (black clear bars). The dotted line shows the difference between the crystal structures expressed as rmsd of ϕ and ψ angles. Arrows indicate residue stretches 10 to 20 and 33 to 44, which show increased flexibility (relative to BPTI) in NMR investigations. LD samples flexibility better than MD in regions 17 to 19 and 33 to 39. Calculation of angle variation is given in Table 1.

which exhibit differences in the crystal structure, are seen to exhibit enhanced angle variation in LD simulations (Fig. 2C). N^{15} relaxation data from NMR investigations of the dynamics of Y35G BPTI have shown a strongly increased flexibility at residues 10–20 and 33–44, which corresponds to motions in the μs to ms time scales [25]. In fact, the NMR data show the predicted increase in mobility at residues 15–20, whereas the crystal structures exhibit small angle variations in this region. The narrow peaks of high mobility in the MD simulation indicate flexibility of single residues or very short stretches that cannot be ascribed to concerted motion of mobile regions. In Fig. 2B the MD simulation shows little mobility

compared to the one from LD simulations. The large dihedral angle variations observed in MD simulations in Fig. 2C reflect local variations of adjacent ϕ/ψ angles but no long-distance correlated dihedral variations. In the case of LD simulations the sausage representation shows long stretches (residues 10–18 and 35–42) of flexibility in correspondence with experimental findings.

The most important finding is that the regions predicted by LD to show the greatest mobility in the mutant are clearly identified with residues shown experimentally to be mobile in the relatively slow μs/ms range which is difficult, if not impossible, to access using conventional MD techniques. The angle variation in MD is relatively low at residues 17–20 and 33–39, underestimating the flexibility identified by NMR in these regions.

Collective motions in the ns time scale have been observed for BPTI in MD simulations in explicit water [21]. LD samples additionally collective motions in the μs to ms time scales using a faster computational scheme.

The average properties of the 100 generated structures of BPTI and Y35G BPTI are summarised in Table 1. The energies of the LD and MD structures are similar, i.e. the difference lies within the standard variation, whereas conformations generated by CED alone are approximately 250 kJ/mol higher in energy. The average radius of gyration is reasonably close to that of the crystal structures in all simulations. The rmsd values and the angle variation values show a similar conformational fluctuation in MD and LD structures of BPTI and less fluctuation in CED structures. The simulations of Y35G BPTI reveal a large backbone variation within the LD conformations and an increased angle variation of the MD and CED structures, compared to BPTI. The ratio of hydrophobic to hydrophilic solvent accessible surface indicates solvation efficiency, since hydrophobic groups tend to be inaccessible in the water environment. The lower values of the ratios for LD structures indicate that the method produces more favourable conformations. Secondary structure assessment indicates an overestimation of β sheet content and an underestimation of helix content in MD simulations, which is not reflected in either LD or CED simulations. The Ramachandran values show few violations for CED simulations, which tend to retain the structures within allowed regions due to their common starting structure and inherent distance geometry constraints. These constraints have a correcting effect on the LD structures (in the CED step), which show fewer disallowed ϕ/ψ values than the MD structures. This trend is also reflected in the more negative PROSA energies, whereas greater WHATIF scores of the MD structures indicate slightly more favourable geometry, probably because the LD conformers retain some of the stereochemical distortions from the CED steps.

4. Conclusions

A novel computational scheme, LD, for the simulation of molecular mobility has been applied to alanine dipeptide and

Table 1
Comparison of average conformational properties of structures generated by MD, LD, CED and reference crystal structures[a] (BPTI, Y35G)

	BPTI MD	BPTI LD	BPTI CED	BPTI	Y35G MD	Y35G LD	Y35G CED	Y35G
E (kJ/mol)[b]	−3975 ± 74	−4039 ± 68	−3758 ± 44	–	−5536 ± 76	−5413 ± 50	−5154 ± 54	–
R_{gyr} (Å)[c]	11.22 ± 0.16	11.03 ± 0.12	11.48 ± 0.05	11.34	10.94 ± 0.11	11.18 ± 0.18	11.53 ± 0.06	10.95
$rmsd^{d}_{bb}$	2.03 ± 0.58	1.98 ± 0.82	1.58 ± 0.49	–	1.93 ± 0.48	2.37 ± 0.59	1.49 ± 0.48	–
$rmsd_{all}$	2.74 ± 0.67	2.49 ± 0.77	1.89 ± 0.57	–	2.60 ± 0.53	3.17 ± 0.69	1.79 ± 0.57	–
Angle variation[e]	23 ± 14	18 ± 5	9 ± 4	–	26 ± 20	31 ± 14	11 ± 3	–
SAS[f]								
SAS_{tot} (Å^2)	4814 ± 73	4699 ± 107	4646 ± 45	4616	4572 ± 97	4702 ± 94	4751 ± 44	4372
SAS_{phob} (Å^2)	2598 ± 50	2497 ± 75	2652 ± 29	2612	2520 ± 58	2553 ± 61	2687 ± 28	2467
SAS_{phil} (Å^2)	2217 ± 41	2202 ± 38	1997 ± 22	2004	2052 ± 52	2150 ± 53	2064 ± 20	1905
SAS_{ratio}	1.17	1.13	1.33	1.30	1.23	1.19	1.30	1.30
Secondary structure[g]								
Helix (%)	17.7	22.6	21.8	20.7	18.2	22.1	22.0	20.7
Sheet (%)	30.3	24.7	24.1	24.1	26.2	17.9	24.1	20.7
Coil (%)	24.9	24.7	28.0	25.9	21.9	30.1	27.4	25.9
Turn (%)	6.8	5.3	5.1	3.4	6.2	7.5	4.9	5.2
Others (%)	20.3	22.7	21.0	25.9	27.5	22.4	21.6	27.5
Rama[h]								
Core (%)	67.3	71.4	86.1	95.7	68.2	69.6	86.5	86.7
Allow (%)	25.6	25.3	13.8	4.3	24.5	28.0	13.3	13.3
Gener. (%)	2.9	1.7	0.1	0.0	1.2	2.0	0.2	0.1
Disallow (%)	4.2	1.6	0.0	0.0	6.1	0.4	0.0	0.0
PROSA[i]	−1.72 ± 0.19	−1.54 ± 0.13	−1.48 ± 0.12	−1.88	−1.33 ± 0.14	−1.23 ± 0.24	−1.44 ± 0.14	−1.52
Z^{j}_{all}	−1.74	−1.80	−1.22	2.03	−1.82	−2.49	−1.54	0.11

[a]Averages are calculated on the basis of 100 structures.
[b]Energy of the molecule in the GROMOS96 force field including implicit solvation terms.
[c]Radius of gyration.
[d]Root mean square deviations of backbone (bb) and all (all) atoms after superposition.
[e]Angle variation is computed as $\sqrt{\sum\{(\Delta\psi^2+\Delta\phi^2)/2n\}}$ values of the sum of ϕ and ψ angle variations.
[f]Solvent accessible surface (SAS) was calculated using a self-written routine; tot, total SAS; phob, hydrophobic SAS; phil, hydrophilic SAS; ratio, ratio of SAS_{phob}/SAS_{phil}.
[g]Secondary structure calculation was performed using MOLMOL.
[h]Ramachandran plot area occupation was determined by use of PROCHECK; core, core area; allow, allowed area; gener., generally allowed area; disallow, disallowed area.
[i]Average energy according to PROSA.
[j]Quality Z-score according to WHATIF.

the proteins BPTI and Y35G BPTI. The results have been compared to those of similar MD and CED simulations and to experimental NMR evidence. Since this method, using an implicit mean solvation, is evidently able to sample conformations corresponding to long-term movements of proteins, it falls in the category of time-saving techniques (cf. [5]). LD achieves sampling of alanine dipeptide conformations that are inaccessible to either MD or CED under the chosen conditions. LD and MD sample molecular motions with apparent differences in sampling performance. This was evident in the case of Y35G BPTI, where the additional flexibility detected by LD corresponds closely to slow motions identified by NMR techniques. This is in marked contrast to the fast motions which are predominantly sampled by MD alone. These results encourage the further development of combined fast sampling/MD methods for application to biological macromolecules, in order to achieve molecular motions on the time scale relevant to biologically important dynamic functions.

Acknowledgements: The authors are grateful to C. Anselmi for the data of the alanine dipeptide map in water, as well as to A. Pastore and S.R. Martin, R. Biekofsky and A. Atkinson for critical reading and helpful suggestions. A shell script for executing LD dynamics is available from the authors upon request.

References

[1] Brooks, C., Karplus, M. and Petitt, B. (1988) Adv. Chem. Phys. 71, 1–259.
[2] Duan, Y. and Kollman, A. (1998) Science 282, 740–744.
[3] Berendsen, H. (1998) Science 282, 642–643.
[4] Caspar, D. (1995) Structure 3, 327–329.
[5] van Gunsteren, W. (1991) AIP Conf. Proc. 239, 131–146.
[6] Fraternali, F. and van Gunsteren, F. (1994) Biopolymers 34, 347–355.
[7] van Schaik, R., Berendsen, H., Torda, A. and van Gunsteren, W. (1993) J. Mol. Biol. 234, 751–762.
[8] Amadei, A., Linssen, A. and Berendsen, H. (1993) Proteins Struct. Funct. Genet. 17, 412–425.
[9] de Groot, B., van Aalten, D., Scheek, R., Amadei, A., Vriend, G. and Berendsen, H. (1997) Proteins Struct. Funct. Genet. 29, 240–251.
[10] Kitao, A., Hayward, S. and Go, N. (1998) Proteins Struct. Funct. Genet. 33, 496–517.
[11] Doniach, S. and Eastman, P. (1999) Curr. Opin. Struct. Biol. 9, 157–163.
[12] Huber, T. and van Gunsteren, W. (1998) J. Phys. Chem. 102, 5937–5943.
[13] Fraternali, F. and van Gunsteren, W. (1996) J. Mol. Biol. 256, 939–948.
[14] Head-Gordon, T., Head-Gordon, M., Frisch, M., Brooks III, C. and Pople, J. (1991) J. Am. Chem. Soc. 113, 5989–5997.
[15] Madison, V. and Kopple, D. (1980) J. Am. Chem. Soc. 102 (15), 4855–4863.
[16] Derremaux, P. and Schlick, T. (1995) Proteins Struct. Funct. Genet. 21, 282–302.
[17] Wlodawer, A., Walter, J., Huber, R. and Sjolin, L. (1984) J. Mol. Biol. 180, 301–329.
[18] Schneider, T., Brünger, A. and Nilges, M. (1999) J. Mol. Biol. 285, 727–740.
[19] Berndt, K., Güntert, P. and Wüthrich, K. (1996) Proteins Struct. Funct. Genet. 24, 304–313.
[20] Smith, L., Mark, C., Dobson, C. and van Gunsteren, W. (1995) Biochemistry 34, 10918–10931.
[21] Hünenberger, P., Mark, A. and van Gunsteren, W. (1995) Proteins Struct. Funct. Genet. 21, 196–213.
[22] Brunne, R., Berndt, K., Güntert, P., Wüthrich, K. and van Gunsteren, W. (1995) Proteins Struct. Funct. Genet. 23, 49–62.
[23] Schiffer, C., Huber, R., Wüthrich, K. and van Gunsteren, W. (1994) J. Mol. Biol. 241, 588–599.
[24] Housset, D., Kim, K.-S., Fuchs, J., Woodward, C. and Wlodawer, A. (1991) J. Mol. Biol. 220, 757–770.
[25] Beeser, S., Goldenberg, D. and Oas, T. (1997) J. Mol. Biol. 269, 154–164.
[26] Hope, H. (1988) Acta Crystallogr. B 44, 22–26.
[27] van Gunsteren, W., Billeter, S., Eising, A., Hünenberger, P., Krüger, P., Mark, A., Scott, W. and Tironi, I. (1996) Biomolecular Simulations: The GROMOS96 Manual and User Guide. ISBN 3 7281 2422 2.
[28] Kabsch, W. and Sander, C. (1983) Biopolymers 22, 2577–2637.
[29] Koradi, R., Billeter, M. and Wüthrich, K. (1996) J. Mol. Graph. 14, 51–55.
[30] Vriend, G. (1990) J. Mol. Graph. 8, 52–55.
[31] Laskowski, R., Moss, D. and Thornton, J. (1993) J. Appl. Crystallogr. 26, 283–291.
[32] Lazaridids, T. and Karplus, M. (1999) Proteins Struct. Funct. Genet. 35, 133–152.
[33] Petitt, B. and Karplus, M. (1988) J. Phys. Chem. 92, 3994–3997.
[34] Beeser, S., Terrence, G. and Goldenberg, D. (1998) J. Mol. Biol. 284, 1581–1596.
[35] Karpen, M., Haseth, P. and Neet, K. (1989) Proteins Struct. Funct. Genet. 6, 155–167.